scientific reports

Check for updates

OPEN

Immunogenicity of intraperitoneal and intranasal liposome adjuvanted VLP vaccines against SARS-CoV-2 infection

Monrat Chulanetra[1], Primana Punnakitikashem[2], Kodchakorn Mahasongkram[1], Wanpen Chaicumpa[1] & Kantaphon Glab-ampai[1]✉

Humans get SARS-CoV-2 infection mainly through inhalation; thus, vaccine that induces protective immunity at the virus entry site is important for early control of the infection. In this study, two anionic liposome (L)-adjuvanted VLP vaccines against SARS-CoV-2 were formulated. Baculovirus-Sf21 insect cell system was used for production of VLPs made of full-length S, M and E proteins. S protein of one vaccine (L-SME-VLPs) contained furin cleavage site at the S1/S2 junction, while that of another vaccine (L-S′ME-VLPs) did not. Both vaccines were innocuous and immunogenic when administered IP and IN to mice. Mice immunized IP with L-SME-VLPs/L-S′ME-VLPs (three doses, two-weeks intervals) had serum virus neutralizing (VN) antibodies (in falling order of isotype frequency): IgG3, IgA and IgG2a/IgG3, IgA and IgM, respectively. The L-S′ME VLPs vaccine induced significantly higher serum VN antibody titers than the L-SME-VLPs vaccine. All mice immunized IN with both vaccines had significant rise of VN antibodies in their bronchoalveolar lavage fluids (BALF). The VN antibodies in 67% of immunized mice were Th1- isotypes (IgG2a and/or IgG2b); the immunized mice had also other antibody isotypes in BALF. The intranasal L-S′ME-VLPs should be tested further step-by-step towards the clinical use as effective and safe vaccine against SARS-CoV-2.

Keywords Baculovirus-insect cell system, COVID-19, Liposome, SARS-CoV-2, Virus-like particles, VLP vaccines, Antibody isotypes

The unprecedented outbreak of human severe pneumonia (later designated COVID-19) caused by severe acute respiratory syngdrome coronavirus 2 (SARS-CoV-2) has spread globally to assume over 200 countries and territories, resulted in 776,618,091 confirmed cases with 7,071,324 deaths since the first case identification in Dec 2019 in Wuhan, China [reported to the World Health Organization based on the WHO Coronavirus (COVID-19) Dashboard on Oct 13, 2024]. Vaccines of different platforms including live attenuated, viral vectored, DNA/RNA-based, protein-based, and inactivated vaccines for parenteral administration (mostly via intramuscular route) have been licensed/authorized for emergency use to cope with the COVID-19 pandemic[1–3], which resulted in reduction of severe morbidity and mortality of the patients and halting community/transcend boundary/global spread of the virus. The pros and cons of these COVID-19 pandemic curbing vaccines have been reviewed[2,3].

SARS-CoV-2 gains body access mainly via upper respiratory tract. The virus can then reach the lower respiratory track and lungs causing severe inflammation including acute respiratory distress syndrome (ARDS)[4]. Intranasal vaccine that engenders protective immune response at the virus entry site is important for early control of the infection and to prevent the virus transmission[5,6]. The mucosal immune system differs in many respects from the systemic counterpart including structure, cellular organization, cellular trafficking, inductive and effector sites, and functional activities of the immunological factors. The mucosal immune response to the administered antigen can occur independently from the systemic immune response[4]. Moreover, immune response elicited at one mucosal inductive site (e.g., nasal associated lymphoid tissue of mice or tonsils in the Waldeyer's ring of human) can be effective at other remote mucosal effector sites, e.g., lungs, intestinal mucosa,

[1]Department of Parasitology, Center of Research Excellence in Therapeutic Proteins and Antibody Engineering, Faculty of Medicine Siriraj Hospital, Mahidol University, Bangkok 10700, Thailand. [2]Department of Biochemistry, Faculty of Medicine Siriraj Hospital, Mahidol University, Bangkok 10700, Thailand. ✉email: kantaphon.gla@mahidol.edu

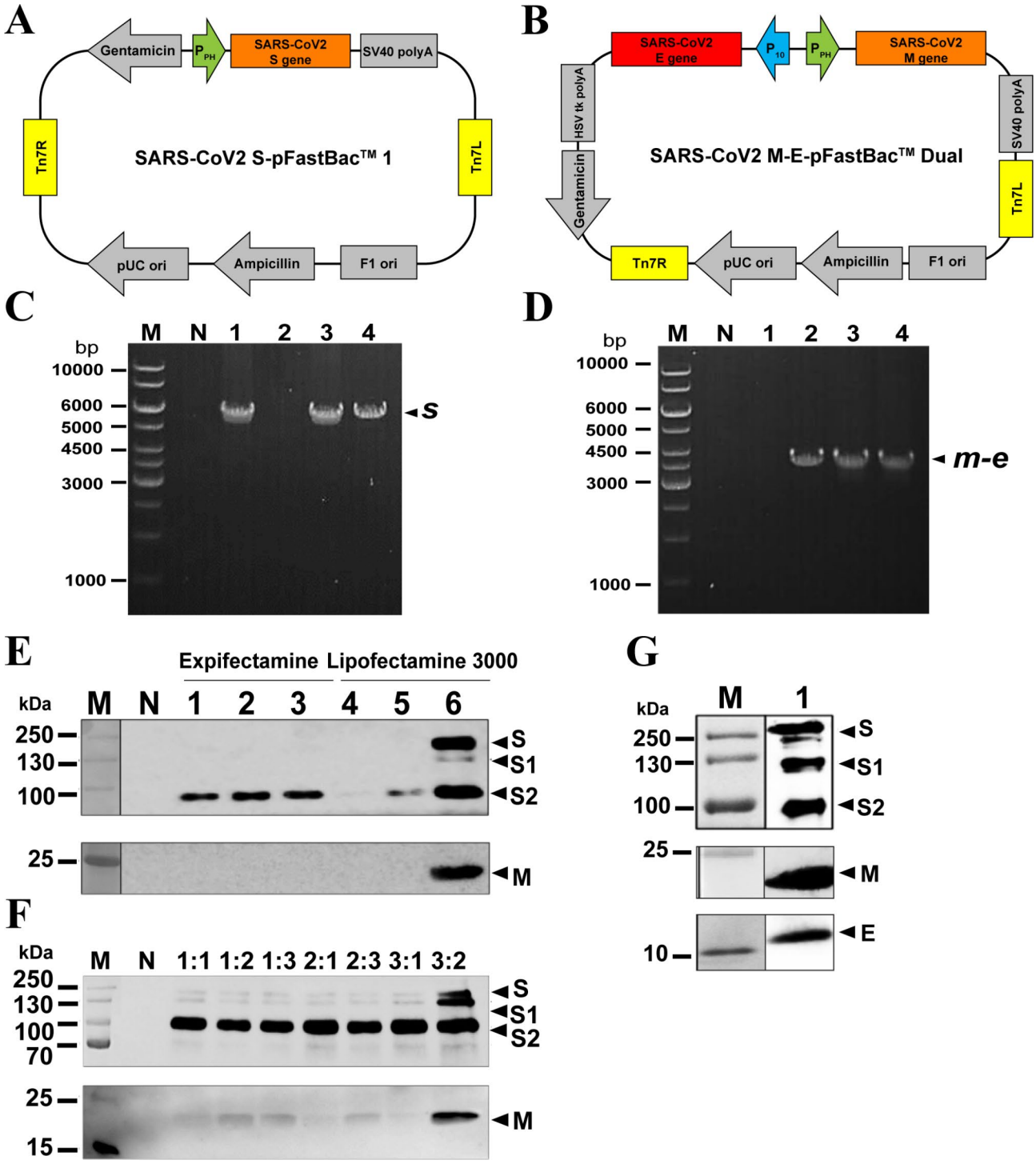

genital mucosa, mammary glands[7]. Parenteral vaccination induces systemic immune responses, but rarely any mucosal immunity[5,8].

An oral/intranasal vaccine against SARS-CoV-2 has been generated. An Adenovirus type 5-vectored SARS-CoV-2 vaccines delivered orally/intranasally to hamsters could reduce disease severity and virus transmission[9]. However, the Adenovirus-vectored vaccine may induce strong immune response to the vector itself rendering poor immunogenicity of the vaccine especially in individuals with high background immunity to the vectored virus. The vaccine cannot be used repeatedly[10]. Besides, the antigen-coding gene delivered by the Adenovirus may be expressed only transiently in transfected cells[10]. An intranasal vaccine containing cationic cross-linked carbon dots (CCD) and RBD-HRs of SARS-CoV-2 (CCD/RBD-HR) induced both systemic and mucosal immunity which protected immunized female BALB/c mice from infections with SARS-CoV-2 Omicron variants[11]. In this study, intranasal vaccines against SARS-CoV-2 made of virus-like particles (VLPs) that consisted of full-length matrix (M), envelope (E) and spike (S) proteins with and without furin cleavage site at the S1/S2 junction were tested for innocuousness and immunogenicity in comparison with the same vaccines administered parenterally (intraperitoneally) to mice, and placebo controls.

◀**Fig. 1**. Panels (**A**) and (**B**) are diagrams of synthetic S-pFastBac1 vector and ME-pFastBac Dual vector, respectively. Panel (**C**) depicts amplicons of SARS-CoV-2 S gene (*s*) in S-pFastBac1 plasmid-transformed MAX Efficiency DH10Bac *E. coli* competent cells; *E. coli* clones 1, 3 and 4 (lanes 1, 3 and 4) were positive for the s amplicons; *E. coli* clone 2 (lane 2) gave negative result. Panel (**D**) shows amplicons of M-E genes (*m-e*) of ME-pFastBac Dual vector-transformed *E. coli* clones; *E. coli* clones 2–4 (lanes 2–4) were positive; *E. coli* clone 1 (lane 1) gave negative *m-e* amplicon. Lanes M of panels (**C**) and (**D**) are DNA markers. Lanes N, Negative DNA controls. Numbers on the left of panels are DNA masses in base pairs (bp). Panel (**E**) shows Western blot patterns of SARS-CoV-2 proteins in culture supernatants of Sf21 cells co-transfected with equal mixtures S-bacmids and ME-bacmids (total amount: 1, 2 and 3 μg) by using Expifectamine or Lipofectamine 3000 (see text for detail). Panel (**F**) are Western blot patterns of SARS-CoV-2 proteins in culture supernatant of Sf21 cells co-transfected with different S-bacmids: ME bacmids ratios (total bacmids amount = 3 μg) by using Lipofectamine 3000. Panel (**G**) are Western blot patterns of SARS-CoV-2 proteins (S, S1 and S2 subunits, M and E) in culture supernatant of Sf21 cells separately transfected with S-bacmids and ME-bacmids (3 μg each). Lanes M of panels (**E**–**G**) are protein molecular weight markers; lanes N is culture supernatant of non-transfected Sf21 cells (negative controls). Numbers on the left of panels (**E**–**G**) are standard protein molecular masses in kDa. The original gels and blots are presented in supplementary Fig. S4.

Results

Generation of recombinant bacmids and baculoviruses for use in VLPs production

Diagrams of the commercially synthesized S-pFastBac1 and ME-pFastBac Dual vectors are shown in Fig. 1A and B, respectively. The synthetic S-pFastBac1 and ME-pFastBac Dual plasmids were used to transform the MAX Efficiency DH10Bac *E. coli* competent cells to generate S-bacmids and ME-bacmids, respectively. PCR amplicons of the S gene (*s*) in the S-bacmids of the *E. coli* clones that were successfully transformed with S-pFastBac1 vector are shown in Fig. 1C; likewise, amplicons of the M-E genes (*m-e*) in the ME-pFastBac Dual vector-transformed *E. coli* clones are shown in Fig. 1D. The S-pFastBac1 vector-transformed DH10Bac *E. coli* clone 1 and the ME-pFastBac Dual vector-transformed DH10Bac *E. coli* clone 2 were grown in large scale and the respective bacmids were extracted for use in P1 baculovirus production.

The Sf21 cells were co-transfected with mixture (equal amount) of the S-bacmids and ME-bacmids using Expifectamine or Lipofectamine 3000 transfection reagent at the total bacmid amounts 1, 2 and 3 μg. It was found that the cells transfected with 3 μg of the bacmid mixture using Lipofectamine 3000 gave the highest amount of recombinant VLP proteins (lane 6, Fig. 1E). Western blot analysis of the culture supernatants containing recombinant P1 baculovirus of the Sf21 cells co-transfected with different ratios of the S-bacmids and ME-bacmids (total 3 μg) using Lipofectamine 3000 are shown in Fig. 1F. The mixture of S-bacmids (1.8 μg) and ME-bacmids (1.2 μg) or ratio 3:2, gave the best yield of S and M proteins. Morphology of the Sf21 cells that were co-transfected with equal amount (3 μg each) of the S-bacmids and ME-bacmids mixture for 24–96 h is shown in supplementary Fig. S3.

Western blot patterns of the S, M and E proteins from culture supernatants of the Sf21 cells separately transfected with 3 μg S-bacmids and 3 μg ME-bacmids using Lipofectamine 3000 are shown in Fig. 1G.

P1 and P2 baculovirus preparations

The concentrations of the P1 baculovirus preparations from co-transfection and separate transfection were determined by focus-forming assay (FFA) before using for P2 baculovirus preparation. The focal characteristics of the Sf21 cells transfected with the S-bacmids and ME-bacmids are shown in Fig. 2.

The concentration of the P1 baculovirus derived from Sf21 cells co-transfected with mixture of S-bacmids and ME-bacmids (3 μg each) (designated SME-P1 baculovirus) was 2.56×10^7 focus-forming units (ffu)/mL. The concentration of the P2 baculovirus prepared from Sf21 cells infected SME-P1 baculovirus (SME-P2 baculovirus) at MOI 0.1 was 4.8×10^8 ffu/mL. The concentrations of P1 baculoviruses from separate transfections with 3 μg S-bacmids (designated S-P1 baculovirus) and 3 μg ME-bacmids (designated ME-P1 baculovirus) were 2.64×10^6 and 9.6×10^6 ffu/mL, respectively. The concentrations of P2 baculoviruses from separate infections with S-P1 baculovirus (S-P2 baculovirus) and ME-P1 baculovirus (ME-P2 baculovirus) were equal, i.e., 5×10^8 ffu/mL.

Because the concentrations and ratio of S-baculovirus and ME-baculovirus in the SME-P2 baculovirus preparation were not known, this preparation was not used further for preparing VLPs. Large scale production of the VLPs was performed by infecting the Sf21 cells with optimal MOI of S-P2 baculovirus and ME-P2 baculovirus. The VLPs were designated SME-VLPs.

Production of virus-like particles (SME-VLPs)

The optimal MOI mixture of the S-P2 baculovirus and ME-P2 baculovirus for SME-VLPs production was determined. Sf21 insect cells were infected with the S-P2 baculovirus and ME-P2 baculoviruses at different mixtures of MOI numbers: 1 and 1, 1 and 5, 1 and 10, 5 and 1, 5 and 5, 5 and 10, 10 and 1, 10 and 5, and 10 and 10. As shown in Fig. 3A, the optimal mixture of baculoviruses was S-P2 baculovirus at MOI 5 and ME-P2 baculovirus at MOI 5 (lane 5) because at this MOI ratio, high amounts of S and M proteins were obtained. Although the MOI number mixture 10 and 1 (lane 7) yielded the highest S protein amount, this MOI number mixture was not chosen because low M protein yield was obtained.

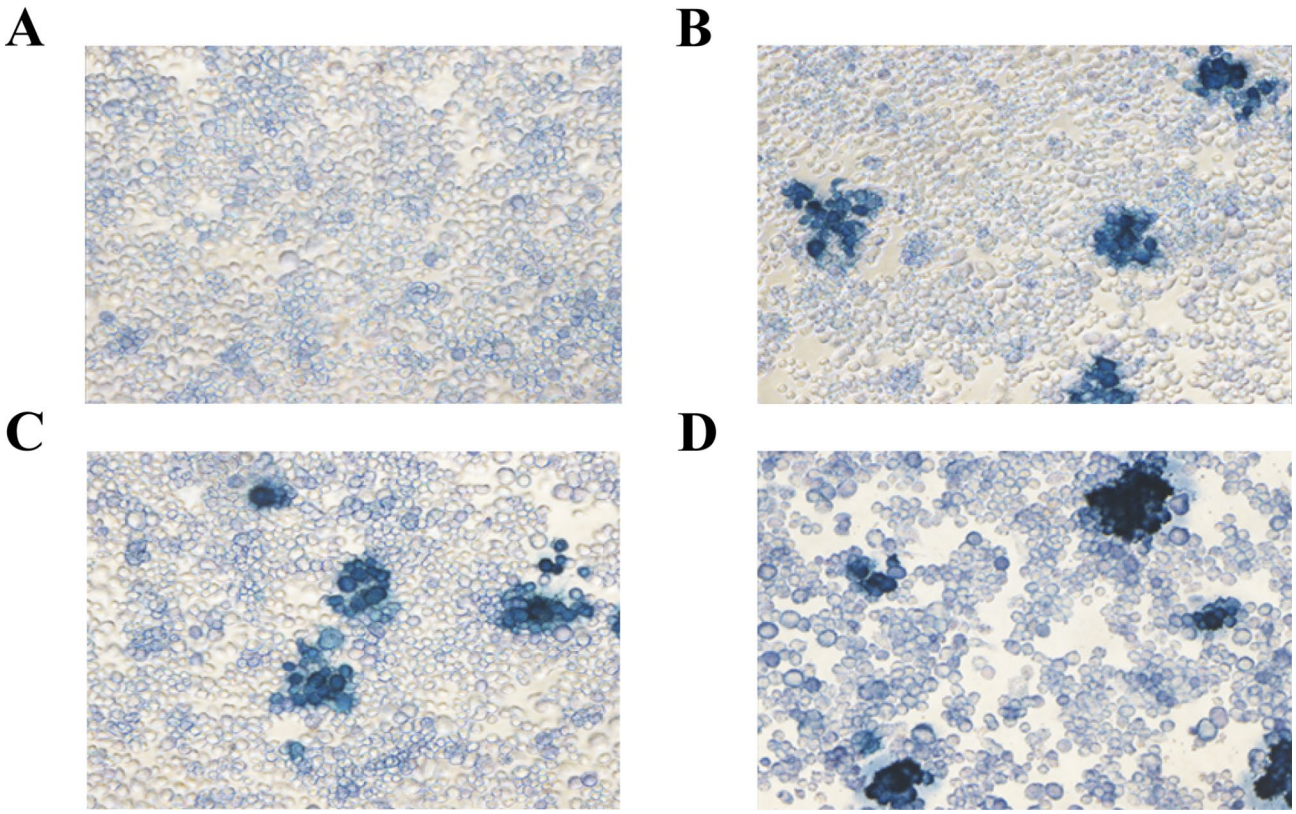

Fig. 2. Foci of Sf21 cells infected with recombinant P1 baculoviruses. Panels (**A**) shows normal Sf21 cells. Panels (**B**), (**C**) and (**D**) show Sf21 cells infected with recombinant S-baculovirus, Sf21 cells infected with recombinant ME-baculovirus, and Sf21 cells infected with recombinant S- and ME-baculoviruses derived from S-bacmids and ME-bacmids co-transfection, respectively.

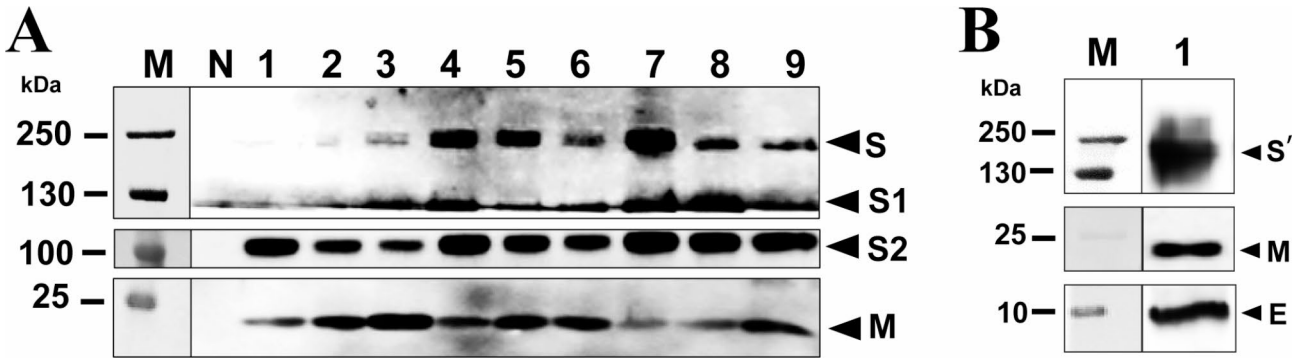

Fig. 3. Production and purification of VLPs. Panel (**A**) are SARS-CoV-2 proteins in SME-VLPs derived from infecting the Sf21 cells with mixtures of S-P2 baculovirus and ME-P2 baculovirus at different numbers of MOI; lanes 1–9 were from MOI 1 and 1, 1 and 5, 1 and 10, 5 and 1, 5 and 5, 5 and 10, 10 and 1, 10 and 5, and 10 and 10, respectively. At the time this experiment was done, the anti-E protein was not available. Panel (**B**) shows Western blot patterns of proteins in the S′ME-VLPs derived from Sf21 cells infected separately with S′-P2 baculovirus at MOI 5 and ME-P2 baculovirus at MOI 5. Lanes M in panels (**A**) and (**B**) are standard protein molecular weight markers. Lane N in panel (**A**) is culture supernatant of non-infected Sf21 insect cells (negative SARS-CoV-2 protein control). The original blots are showed in supplementary Fig. S5.

Production of VLPs that their displayed S protein did not have furin cleavage site at the S1/S2 junction (S′ME-VLPs).

The S′ME-VLPs were prepared using the same protocol as for the SME-VLPs but the plasmid S′-pFastBac1 containing inserted SARS-CoV-2 S gene without furin cleavage site at the S1/S2 junction (*s′*) was used for generation of the S′-bacmids and the production of the S′-P1 baculovirus and S′-P2 baculovirus. The S′ME-

VLPs contained intact S (without cleavage products: S1 and S2 subunits), M and E proteins as shown in Fig. 3B. The SME-VLPs and S′ME-VLPS were purified by using HiTrap Capto CORE 400 columns.

Characteristics of SME-VLPs, S′ME-VLPs, liposome-adjuvanted SME-VLP (L-SME-VLP) vaccine, liposome-adjuvanted S′ME-VLP (L-S′ME-VLP) vaccine, and liposome-entrapped PBS (L-PBS; placebo)

Morphology SME-VLP (as a representative) revealed by TEM is illustrated in Fig. 4A. The particle shows an envelope membrane with a few intact spikes. Particle size (Z-average) and zeta potentials and particles size of the VLPs and liposome-encapsulated VLPs are detailed in Fig. 4B–F; Table 1. They were all anionic micelles.

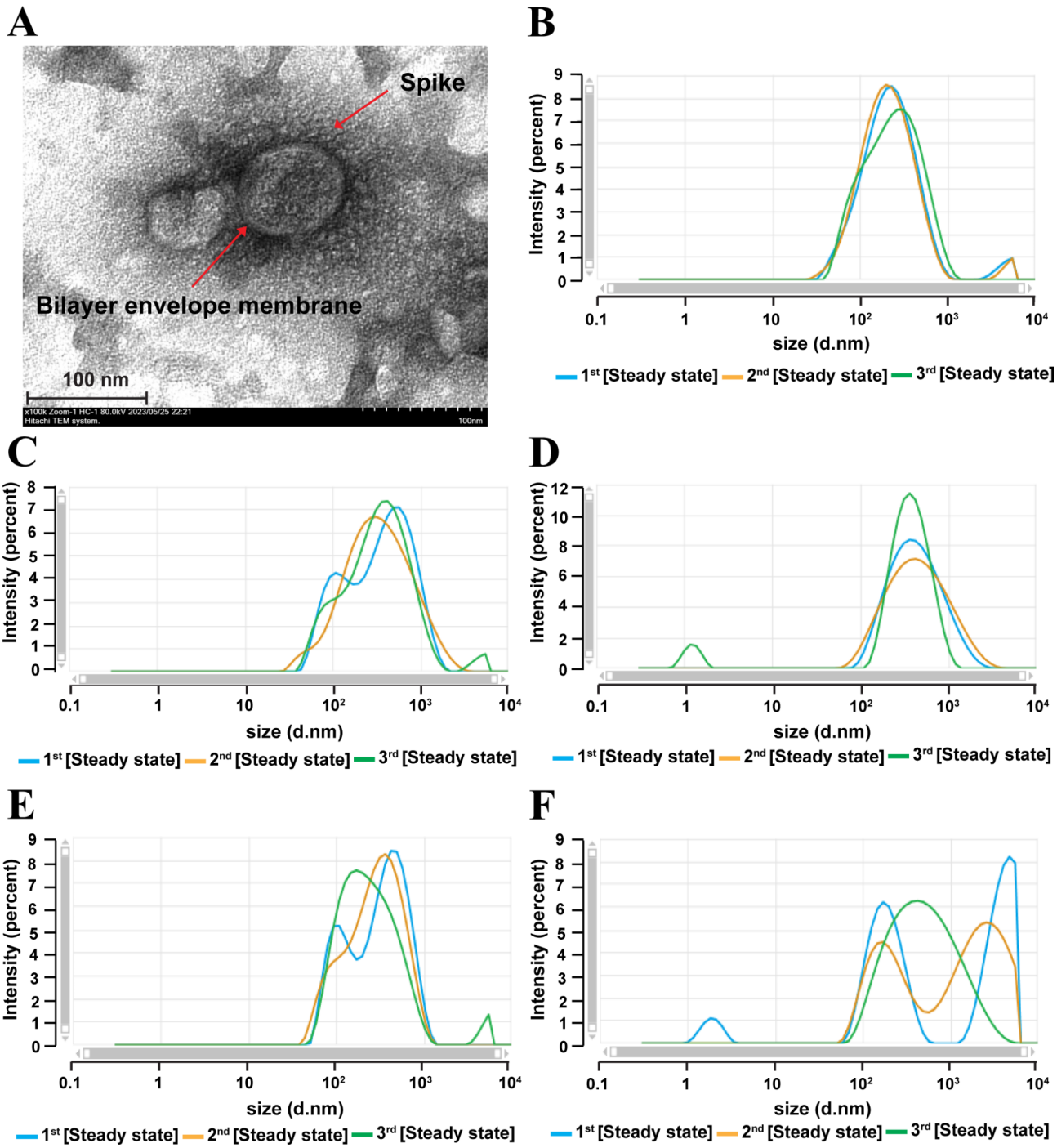

Fig. 4. Characteristics of VLPs. Panel (**A**) shows morphology of the representative SME-VLP. Panels (**B**–**F**) demonstrate sizes of the SME-VLPs, S′ME-VLPs, liposome-encapsulated SME-VLPs (L-SME-VLP), liposome-encapsulated-S′ME-VLPs (L-S′ME-VLP), and liposome-entrapped PBS (L-PBS), respectively.

Particles	Zeta potential (mV)	Conductivity	Wall-size potential (mV)	Quality factor
SME-VLPs	−1.96	0.287	0	1.03
S′ME-VLPs	−5.31	0.278	0	1.20
L-SME-VLPs	−5.12	0.289	−7.14	1.43
L-S′ME-VLPs	−18.63	0.291	−20.1	1.83

Table 1. Zeta potentials of the VLPs and liposome-encapsulated VLPs.

Innocuity and immunogenicity of the liposome-adjuvanted VLP vaccines

Mice injected intraperitoneally (IP) or administered intranasally (IN) with the L-SME-VLP or L-S′ME-VLP vaccines did not show any sign of vaccine-related adverse effects; their internal organs showed normal gross appearance similar to the control mice that received placebo (L-PBS), indicating innocuousness of the vaccines. Representatives of the internal organs of mice of all treatment groups are shown in Fig. 5.

Levels of antibodies in serum samples and bronchoalveolar lavage samples (BALF) of mice immunized IP and IN with L-SME-VLP and L-S′ME-VLPs are shown in Fig. 6 and Table S1. Both vaccines were highly immunogenic, i.e., induced systemic immune response (serum antibodies by indirect ELISA) when administered IP (Fig. 6A) and IN (Fig. 6B). The L-S′ME-VLP vaccines induced significantly higher serum virus neutralizing (VN) antibody titers than the L-SME-VLP vaccine (Fig. 6C). Both vaccines induced VN antibody titers in BALF samples of the immunized mice (Fig. 6D), but negligible serum ELISA titer against S1 protein (two independent and reproducible experiments). None of the control mice had detectable ELISA/VN antibodies to SARS-CoV-2 S1 protein (data not shown).

Immunoglobulin isotypes of the antibodies in the immunized mouse samples are shown in Fig. 7 and Table S2. All antibody isotypes carried κ light chains.

Serum samples of 5/6 mice (83%) that received L-SME-VLP (T2-T6) and L-S′ME-VLP (T7-T11) vaccines intraperitoneally (IP) had IgG3. Three and two mice of the L-SME-VLP IP group had serum IgA (T1-T3) and serum IgG2a (T2 and T4). Two mice and one mouse of the L-S′ME-VLP IP group had serum IgA (T10 and T12) and serum IgM (T12).

Sixty percent (4/6) of mice that were immunized intranasally (IN) with L-SME-VLP (T14, T15, T17 and T18) or L-S′ME-VLP (T19-T22) vaccines had Th1-antibody isotypes, i.e., IgG2a and/or IgG2b in their BALF samples. For the L-SME-VLP IN group, two mice each had BALF IgG3 (T13 and T16) and BALF IgA (T16 and T18), and one mouse each had BALF IgM (T15) and IgG1 (T18). Two mice and one mouse of the L-S′ME-VLP group had BALF IgG3 (T22 and T23) and IgM (T24).

Cytokine profiles in spleens of immunized and placebo mice are shown in Fig. 8. Mice immunized IP with L-S′ME-VLPs had high expressions of cytokines genes compared to control mice including Th1 (IL-2, IFN-γ and TNF-α), Th2 (IL-4, IL-5, IL-10, IL-13), IL-17 and TGF-β (Fig. 8A). Mice immunized IP with L-SME-VLPs had a significant rise of only IFN-γ gene compared to control mice.

Mice immunized IN with L-S′ME-VLPs had significantly higher expressions of genes coding for TNF-α, TGF-β, IL-2, IL-4, IL-10, IL-13, and IL-17 while mice immunized IN with L-SME-VLPs had only a rise in mRNA expression of IL-17 gene, compared to placebo mice (Fig. 8B).

Discussion

Intranasal vaccination can confer protection against pathogens that enter the host's body via repiration. In this study, anionic liposome adjuvanted vaccines made of SARS-CoV-2-like particles administered via intranasal route induced significant rise of virus neutralizing antibodies in the brochoalveolar lavage fluids of the vaccinated mice.

From co-transfection and separate transfection of Sf21 cells with S-bacmids and ME-bacmids, the Western blot analysis of the culture supernatants of the transfected cells containing P1 baculoviruses revealed relatively small amount of intact S protein with apparent molecular size of approximately 250 kDa, and the cleaved S products, i.e., the S1 and S2 subunits which the apparent molecular sizes were approximately 100–120 and 70–100 kDa, respectively. Theoretically, the nascent S, S1 and S2 proteins (without post translational modification) of the SARS-CoV-2 wildtype strain are 141.2, 75.3 and 58–60 kDa, respectively[12]. The molecular sizes of the intact S protein and the S1 and S2 subunits may vary from the theoretical molecular weights due to post translational modifications, post translation cleavages, relative charges, and other experimental factors[13,14]. The post-translational modification of the recombinant S protein in the insect cells accounted for the apparent larger sizes of the S and its subunits of this study.

The S′-P1 baculovirus derived from Sf21 insect cells separately transfected with S′-bacmids and ME-bacmids showed intact S protein and no S1 and S2 subunits in Western blot analysis. Thus, the S′-P2 baculovirus and S′ME-VLPs derived from the S′-P1 baculovirus should also carry intact S protein. In this study, immunogenicity of the anionic liposome-adjuvanted vaccines consisting of VLPs expressing M, E and S/S′ proteins (L-SME-VLP and L-S′ME-VLP, respectively) were investigated. The two vaccines were immunogenic in inducing systemic and mucosal immune responses.

The VLPs of this study mimic the structural organization and conformation of the authentic native SARS-CoV-2 particles but lacking the viral ribonucleoprotein (RNP)[15]. The SME-VLPs and the S′ME-VLPs (without including the length of the spike projections) were approximately 179 and 207 nm in median diameters, respectively, which are conformed to the size of the commercialized SARS-CoV-2 VLPs produced from transfected HEK293 cells[16]. The median size of the authentic native SARS-CoV-2 particles without spikes was

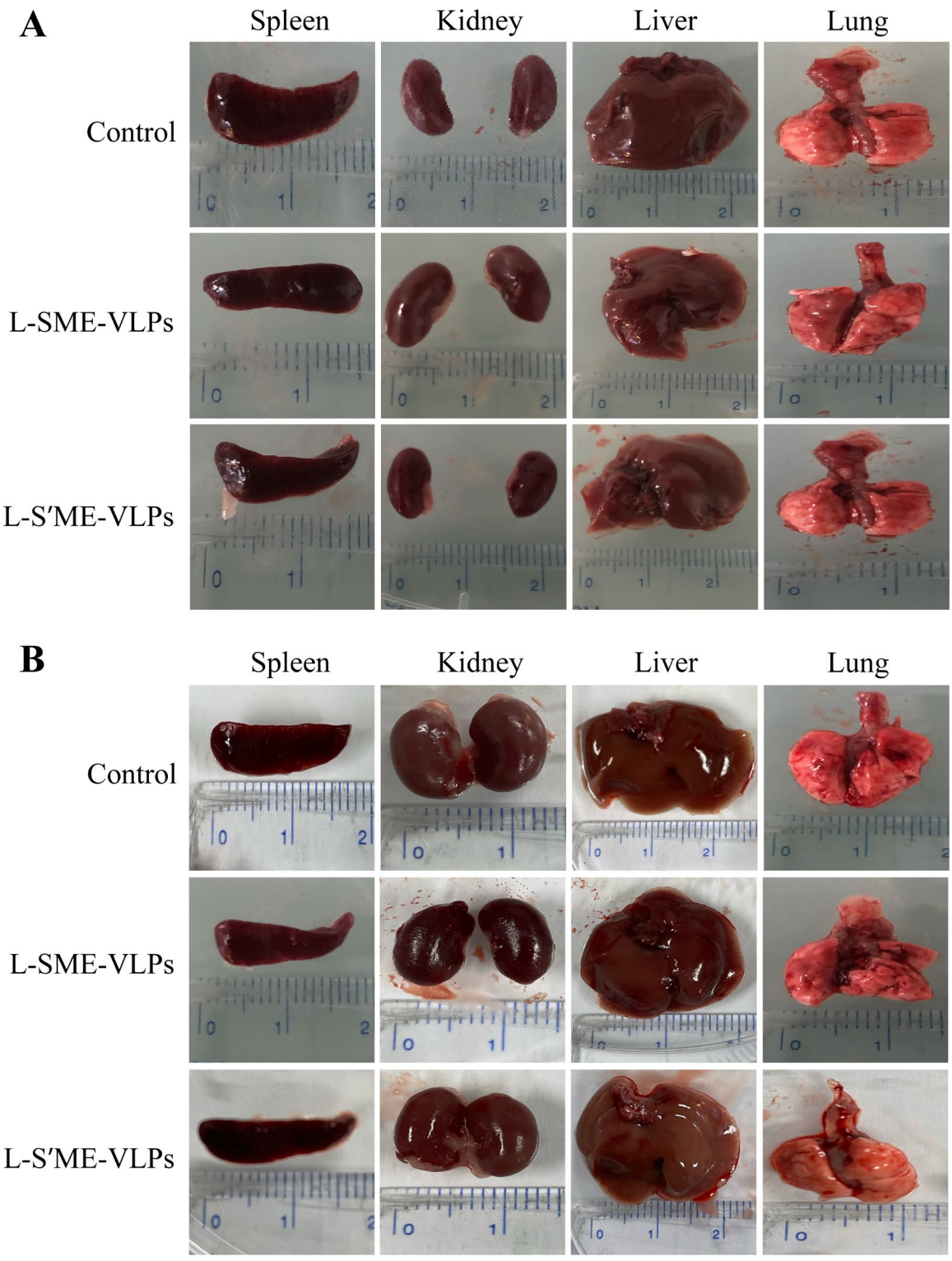

Fig. 5. Gross appearances and sizes of internal organs of immunized and control (placebo) mice. Panel **A**, Intraperitoneally immunized and control mice. Pabel **B**, Intranasally immunized and control mice.

100 nm[17]. After being encapsulated by liposome (L), the median sizes of the liposome-encapsulated SME-VLPs (L-SME-VLP vaccine) and S′ME-VLPs (L-S′ME-VLP vaccine) were 316 and 237 nm in the average, respectively, which were not significantly different from the average size of the liposome-entrapped PBS (placebo; L-PBS; 342 nm). The correlation of the particulate adjuvant characteristics (including sizes and surface charges) with the resultant immune responses against the adjuvanted vaccines has been reviewed extensively[18]. The size of the particulate adjuvants may have different effects on the type of the vaccine-induced immune responses. For

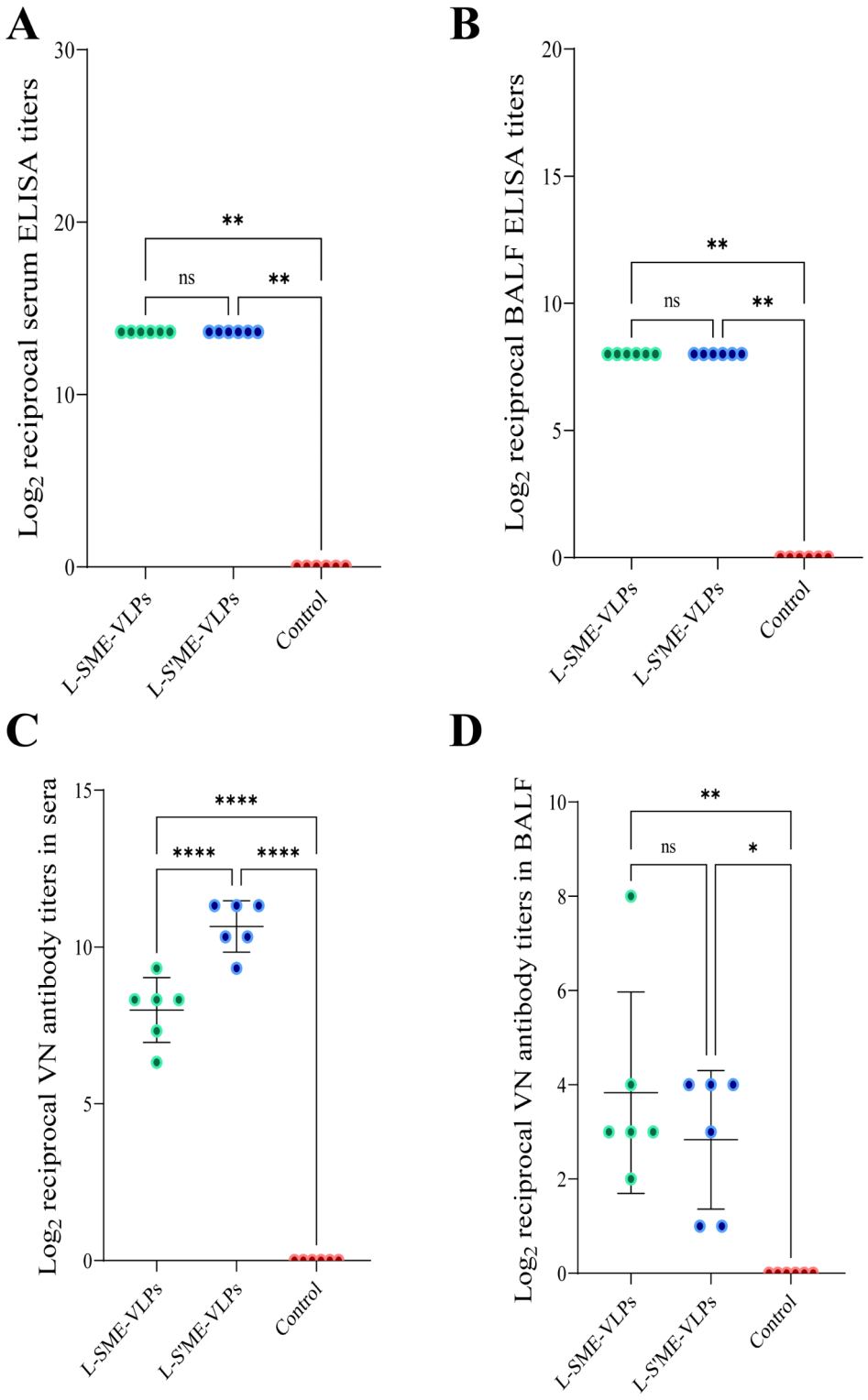

Fig. 6. Indirect ELISA and virus neutralizing (VN) titers in samples of immunized mice.

targeted-delivery systems, nanoparticles (1–1000 nm) are considered more effective than microparticles (1–1000 μm), as the former is more efficient in diffusing through biological barriers, passing through capillaries and being relatively stable in blood circulation[18–20]. For vaccines, however, experimental results pertaining to the optimal size ranges of the particulate-based delivery system that will generate strong and sustained immune responses to the co-administered antigen are conflicting[18,21]. Nevertheless, evidence indicated that immunization with the 200–600 nm particles favored Th1 immune responses, whereas immunization with the 2–8-μm particles favored Th2 response[22]. For respiratory infections, like respiratory syncytial virus (RSV) and SARS-CoV/SARS-

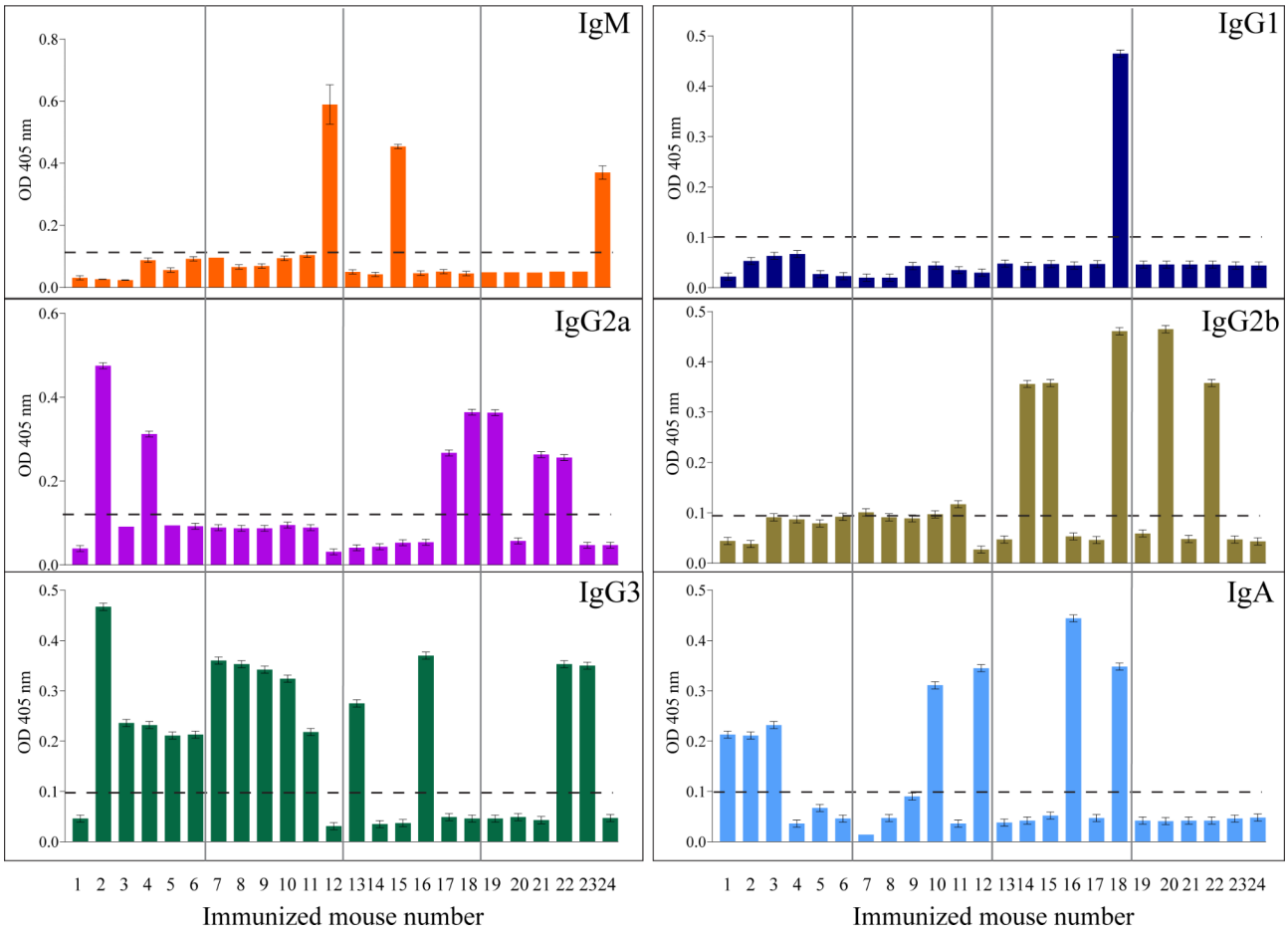

Fig. 7. Immunoglobulin isotypes of antibodies in the immunized mouse samples. Dotted lines are arbitrary cut-off OD 405 nm between positive and negative ELISA results.

CoV-2, Th1 response to vaccine is preferred to the Th2 response as it was observed in vaccinated animal models as well as in children that the Th2 response may exacerbate lung inflammation upon experiencing new infection due to immunopathology that reminiscent the type 1 hypersensitivity with eosinophil infiltration and immune complex deposition in the lung[23,24].

Both SME-VLPs and S′ME-VLPs of this study carried negatively charged surface (-1.96 and −5.31, respectively). After liposome encapsulation, the negative charges of the vaccine micelles were increased to -5.12 and −18.63, respectively. The anionic liposome-adjuvanted VLP vaccines (L-SME-VLPs and L-S′ME-VLPs) were administered intraperitoneally (IP) or intranasally (IN) to mice. In the peritoneal cavity, macrophages (that functions in immune surveillance against invader) effectively detect, phagocytose, and process the antigen for T cell presentation and B1 cell stimulation. At the mucosal surface, like nasal cavity and intestine, the mucin glycoproteins in the mucus gel layer carry strongly net-negative surface due to their high sialic acid and sulfate content[39]. Thus, for the mucosal vaccination, anionic or neutral nanoparticles/liposome with encapsulated immunogen will not bind to or trapped in the negatively charged mucosa, allowing them to be easily approachable, endocytosed, and transported by microfold/M cells to the inductive site of the respective mucosal lymphoid tissue, such as, mouse organized and diffuse nasal-associated lymphoid tissues (ONALT and DNALT), tonsils, Peyer's patches, draining lymph nodes[25]. Thus, negatively charged carriers may favor mucosal vaccination such as intranasal, oral, or vaginal vaccination[25–27].

Although intraperitoneal route of immunization is not in medical practice, however, intraperitoneal immunization of mice has been utilized extensively in research for vaccine development against respiratory viruses, including influenza virus, respiratory syncytial virus (RSV), and SARS-CoV-2 vaccines, to gain primary data on innocuity and immunogenicity[28–30]. Intraperitoneal inoculation with live influenza A virus confers protection against intranasal infections in mice and ferrets[29]. Intraperitoneal immunization induced acute and memory immune responses capable of effector functions and protection at distal nasal mucosa and lung against RSV[28]. Intraperitoneal immunization was performed in this study for testing innocuousness and immunogenicity of the anionic liposome-adjuvanted VLP vaccines against SARS-CoV-2. Mice immunized intraperitoneally (and intranasally) with both vaccines did not show any sign of vaccine related adverse effect. Gross appearances of the internal organs of the immunized mice at the end of the experiments were not different from the control mice that received placebo. The peritoneal cavity is the largest serosal body space that harbors most of the abdominal

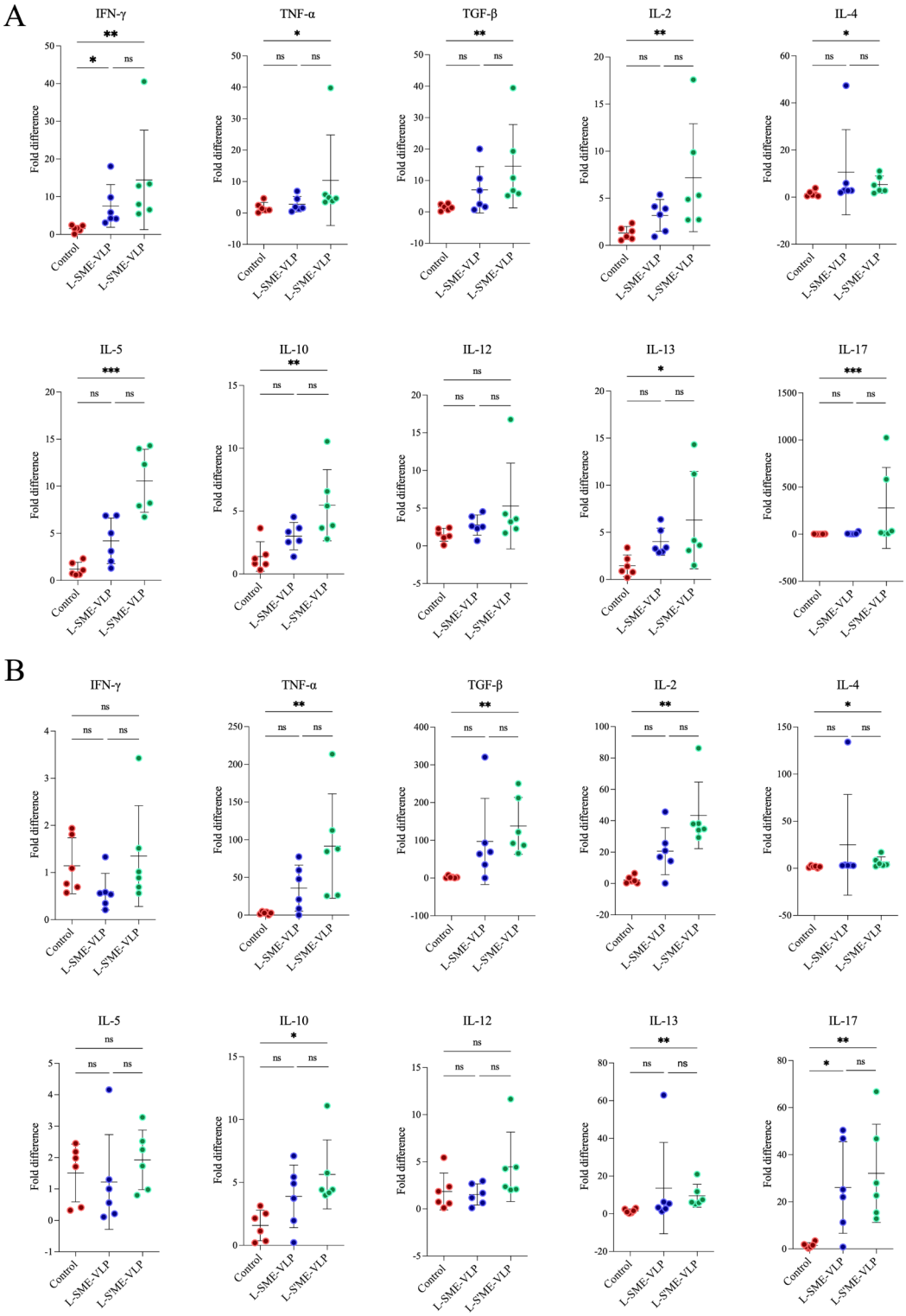

Fig. 8. Fold differences of cytokine mRNAs in spleens of immunized mice relative to control (placebo) mice. Panel (**A**), intraperitoneally immunized mice. Panel (**B**), intranasally immunized mice.

organs and an important visceral adipose tissue called omentum. The omentum contains milky spots which are clusters of leukocytes that the cells are organized like those in the secondary lymphoid tissues, i.e., a central B cell area surrounded by T cells and myeloid cells that are supported by a fibroblastic stromal cell network[31,32]. The omentum (and other serous cavities, e.g., pleural cavity) is a site of B1 cell lymphopoiesis and T cell-independent immune responses to multivalent antigens. B1 cells produce cross-reactive antibodies that are mainly IgM but can be IgG3 and IgA isotypes[33]. Besides, activated B1 cells can migrate to mucosal surface such as intestinal

lamina propria and differentiate into plasma cells that secrete IgA antibodies for protection of the mucosal surface[34]. Activated B1 cells can migrate to spleen where they serve as precursor of splenic IgM producing cells[35]. Peritoneal B1 cells can switch readily to antibody producing cells in splenic marginal zone[36].

After three IP doses of the L-SME-VLP/L-S′ME-VLP vaccines, the titers of the ELISA antibodies to SARS-CoV-2 S1 subunit and VN antibodies were markedly rised, indicating vaccine immunogenicity. Unfortunately the end-point serum ELISA antibody titers of the vaccinated mice (tested in triplicate) could not be reached and the experiments could not be repeated due to limited quantity of the samples. From microneutralization assays, however, the L-S′ME-VLP (the S′ protein displayed on the VLP surface lacks furin cleavage site at the S1/S2 junction) induced significantly higher serum VN antibody titers than the L-SME-VLP vaccine. This might be because the former had more of the intact S1 subunit[37], hence, more S1 neutralizing epitopes especially on the RBD. The magnitude of systemic immune responses in mice immunized IP with the vaccines coinsided with the cytokine responsive profiles in spleen; i.e., the L-S′ME-VLPs induced high expressions of both Th1 and Th2 cytokine genes than the L-SME-VLPs.

The predominant isotype of the serum anti-S1 antibodies of 5 of 6 immunized mice (83%) were IgG3 which can be either from activated B1 cells that migrated to other lymphoid tissues, i.e., spleen and lymph nodes, or from the activated B2 cells in the peripheral lymphoid tissues in response to the vaccine immunogen that entered systemic circulation. Mouse IgG3 is highly efficient in complement activation, opsonophagocytic activities as well as antibody-dependent cell-mediated cytotoxicity (ADCC)[38] which cause virus clearance upon infection. Nevertheless, complement fixation and immune-complex formation may exacerbate the inflammation and cytokine storm as well as causing infiltration of inflammatory cells (especially eosinophils) into lungs of the virus infecting host which exacerbates the critical morbidity[23,39].

The upper respiratory tract is an important prime site of host defense against inhalant pathogens, e.g., respiratory viruses like influenza virus, RSV and SARS-CoV-2. Advantages of intranasal vaccination in induction of the mucosal and systemic immunity have been reviewed[39]. Intranasal immunization effectively induces protective immunity by triggering both mucosal and systemic responses following antigen administration which contrasts with intramuscular injection that primarily induces systemic immune responses[40,41]. Intranasal vaccination can confer protection against infections at other mucosal sites, such as the lower respiratory tract and lungs, intestines, and genital tract, and may provide cross-protection against variant strains due to cross-reactive/poly-reactive nature of antibodies produced by activated B1 cells[42]. Three doses of the L-SME-VLP and L-S′ME-VLP vaccines containing 30 μg VLPs/dose, administered intranasally at two-weeks intervals did not induce significant rise of serum antibodies, although there were a significant increase of spleen cytokine expressions in L-S′ME-VLPs immunized mice such as TNF-α, TGF-β, IL-2, IL-4, IL-10, IL-13 and IL-17 (IL-17 only in L-SME-VLPs immunized mice), indicating that the immunizing dose might be too low, or the time of sample collection was too soon[43]. Both vaccines were found to induce predominantly Th1 response as shown by IgG2a and/or IgG2b antibody isotypes in the BALF, and less IgG3. Two of five mice (40%) immunized with L-SMS-VLP vaccine had IgA response. IgG2a and IgG2b are relatively poor in complement activation and opsonophagocytic activities compared to the IgG3[44]. On contrary, several studies have demonstrated that specific IgG2a exhibits stronger anti-viral effects than other antibody isotypes[45–48]. Predominant IgG2a among many IgG antibody responses elicited by live viruses could confer the best protection for the infected host[49]. Usually, secretory IgA is the signature of mucosal adaptive immune response against invading pathogens. Secretory IgA exerts first line defense against invading pathogens at the portal of entry. Induction of antigen-specific IgA at the mucosa is regulated by the nature of antigen (T-independent vs. T-dependent), IgA-producing cytokines (e.g., TGF-β, IL-1, IL-4, IL-6, IL-10 and IL-21) and other co-stimulatory signals (such as B cell-activating factor of TNF family or BAFF, a proliferation-inducing ligand or APRIL, retinoic acid, nitric oxide) in the mucosal-associated lymphoid tissue (MALT) that contribute to B cell Ig class-switching[49]. For a mucosal vaccine to induce high titer mucosal IgA, a delivery system that facilitate antigen-uptaking by antigen-presenting cells (APCs) or M cells, such as by adding APC/M cell-surface targeting molecule, and adjuvant that enhances APCs to express costimulatory molecules (CD80/86, OB40L, 4-1BBL, GITRL), MHC class II, and IgA-inducing cytokines should be adopted[50]. The intranasal route of vaccination should be well suited for pandemic/epidemic control of highly contagious/infectious respiratory viruses following the outbreak, because it is relatively easy to do; thus, less skilled personnels can be recruited for doing the mass vaccinations[47]. The intranasal route causes minimal discomfort with no intrusive and pain; therefore, it should receive better compliance from children, needle-fear subjects, and patients with morbidities that required multiple/frequent injections[44,51].

In conclusion, both vaccines induced principally serum IgG3 antibody isotype response in the intraperitoneally immunized mice while mice immunized intranasally with the vaccines had principally Th1-type response as shown by predominant IgG2a and/or IgG2b antibody isotypes in the bronchoalveolar lavage fluids. The vaccine formulation could be modified for induction of high mucosal IgA VN titer. Limitations of this study are the lack of the vaccines' protective data from SARS CoV-2 animal models of infection, e.g., hamsters and transgenic K18-hACE2 mice. Also, cross-protection of the vaccine-induced immune responses against heterologous SARS-CoV-2 variants should be performed. Thus, the intranasal anionic liposome-adjuvanted VLP vaccines require testing further step-by-step towards the clinical use as an effective, safe and well-compliant vaccine that induces the first line defense against the inhalant SARS-CoV-2.

Materials and methods

Cells, media, bacteria, viruses, and virus propagation

Sf21 insect cells (Catalog number: 11497013) were from Invitrogen, Thermo Fisher Scientific, Waltham, Massachusetts, USA. Sf-900 III serum-free medium was from Thermo Fisher Scientific (Catalog number: 12658027). Super optimal broth with catabolite repression (SOC) was from Invitrogen, Thermo Fisher Scientific (Catalog number: 15544034). Dulbecco's modified Eagle's medium (DMEM) was from Gibco, Thermo Fisher

Scientific (Catalog number: 11965092). Fetal bovine serum (FBS) was from Hyclone, Cytiva, Marlborough, USA (Catalog number: SH30071.03). MAX Efficiency DH10Bac *Escherichia coli* competent cells containing Autographa californica Multiple Nuclear Polyhedrosis Virus (AcMNPV) Bacmids were from Invitrogen by life technology, Thermo Fisher Scientific (Catalog number: 10361012).

SARS-CoV-2 virus, Wuhan strain Si01 was propagated in the Vero E6 cells. The Vero E6 cells (5×10^6 cells) were seeded to T75-flasks (Nunc, Thermo Fisher Scientific, Catalog number: 178905) and incubated overnight at 37 °C in 5% CO_2 atmosphere. The flasks were moved to biosafety level 3 (BSL-3) laboratory, Department of Microbiology, Faculty of Medicine Siriraj Hospital, Bangkok. The SARS-CoV-2 was diluted in DMEM and added to the Vero E6 cells at MOI 0.1. The infected cells were incubated at 37 °C in 5% CO_2 atmosphere for 1 h; the supernatant was removed, and the DMEM supplemented with 2% FBS was added to the infected cells and incubated in 37 °C, 5% CO_2 incubator for 72 h. The preparation was centrifuged; the SARS-CoV-2 concentration in the cell-free supernatant was titrated by plaque-forming assay (PFA)[52]. The virus was kept at -80 °C until use.

Preparation of recombinant bacmids

Full-length gene sequences coding for S, M and E of SARS-CoV-2 Wuhan-Hu-1 (GenBank accession no. MN908947.3) were used for generation of recombinant plasmids, including recombinant S-pFastBac1 and ME-pFastBac Dual vectors (GenScript, Piscataway, NJ, USA). One nanogram of each recombinant vector was mixed with 100 µL of log-phage grown MAX Efficiency DH10Bac *E. coli* competent cells in separate tubes. The tubes were placed in ice-bath for 20 min, then transferred to 42 °C water-bath for 45 s, and ice-bath for 2 min (heat-shock transformation). Competent cell recovery medium (Super optimal broth with catabolite repression (SOC; 900 µL) was added to each tube and incubated at 37 °C with shaking aeration (225 rpm) for 4 h. Each preparation was then diluted 10-fold serially; each dilution (100 µL) was spread onto Luria-Bertani (LB) agar plates containing antibiotics [50 µg/mL kanamycin (Kangen, Bangkok, Thailand, Catalog number: 1A158/29), 7 µg/mL gentamycin, and 10 µg/mL tetracycline (AppliChem GmbH, Damstadt, Germany, Catalog number: A1492.0025 and A2228.0025, respectively), 100 µg/mL Blue-Gal (Abcam, Cambridge, USA, Catalog number: ab146379) and 40 µg/mL isopropyl β-d-1-thiogalactopyranoside (IPTG) (Vivantis Technologies, Selangor Darul Ehsan, Malaysia, Catalog number: PC0708-5 g). The plates were incubated at 37 °C for 48 h. White colonies were streaked on fresh LB agar plates containing the antibiotics and Blue-Gal for the colonies' verification. The transformed DH10Bac *E. coli* colonies with respective recombinant bacmids (derived from transposition of S, M and E genes from S-pFastBac1 and ME-pFastBac Dual plasmids to bacmids in *E. coli*; as shown by diagram in supplementary Fig. S1) were checked by PCR using pUC/M13 forward primer: 5′CCCAGTCACGACGTTGTA AAACG3′ and pUC/M13 reverse primer: 5′-AGCGGATAACAATTTCACACGG-3′.

The recombinant bacmids, designated S-bacmids and ME-bacmids, were extracted from the respective PCR-positive DH10Bac *E. coli* clones by using PureLink HiPure Plasmid DNA Purification kit (Invitrogen, Thermo Fisher Scientific, Catalog number: K2100-06). *Escherichia coli* colonies were grown in 5 mL LB broth containing antibiotics at 37 °C with shaking aeration (250 rpm) overnight. Individual cultures were added to 500 mL of fresh LB broth, incubated overnight, and centrifuged (4500 × *g*, 30 min). Each bacterial pellet was resuspended in a 10 mL R3 buffer (buffers and columns were provided with the plasmid DNA purification kit) before adding with 10 mL L7 lysis buffer. The tubes were inverted several times and kept at room temperature (25 ± 2 °C) for 5 min, added with 10 mL N3 precipitation buffer, mixed well, and centrifuged (11,000 × *g*, 4 °C, 15 min). Supernatants were loaded to separate columns; the columns were equilibrated with Eq. 1 buffer, and the samples were allowed to flow through, followed by washing each column with 60 mL W8 buffer. The bacmids were eluted with 15 mL E4 elution buffer; each eluate was added with 10.5 mL isopropanol, and centrifuged (11,000 × *g*, 4 °C, 15 min). Supernatants were discarded; the pellets containing bacmids were washed thrice with 70% ethanol and finally suspended in 500 µL Tris-EDTA (TE) buffer (10 mM Tris-HCl containing 1 mM EDTA·Na_2). Bacmid DNA amounts were determined by nanodrop (Thermo Fisher Scientific).

Preparation of P1 and P2 baculoviruses

For preparing P1 baculovirus, Sf21 cells were transfected with either mixture of the S-bacmids and ME-bacmids (co-transfection) or transfected separately with the S-bacmids and ME-bacmids (separate transfection).

For the co-transfection, Sf21 cells were seeded into 6-well culture plates (1×10^6 cells in 2 mL Sf-900 III SFM medium/well) and the plates were kept at 27 °C, non-CO_2 atmosphere and non-humidified in New Brunswick S41i incubator shaker (Eppendorf, Hamburg, Germany) for 1 h. Two types of transfection reagents were used for the cell transfection: Expifectamine Sf transfection reagent (Gibco, Thermo Fisher Scientific, Catalog number: A38915) and Lipofectamine 3000 transfection reagent (Thermo Fisher Scientific, Catalog number: L3000008). The S-bacmids and ME-bacmids were mixed (equally at total bacmid amounts 1, 2, 3 µg) and added separately to 10 µL of the Expifectamine transfection reagent in 250 µL of Opti-MEM I reduced serum medium (Invitrogen, Catalog number: 31985070). The preparations were kept at room temperature for 5 min before adding to appropriate wells containing Sf21 cells. For transfection using Lipofectamine, individual bacmids (1, 2, 3 µg) were mixed with 5 µL of P3000 in 125 µL of Opti-MEM I reduced serum in a tube (tube A). In another tube (tube B), 5 µL of Lipo-3000 and 117.5 µL of Opti-MEM I reduced serum were mixed. The contents of both tubes were combined, kept at room temperature for 15 min, and added to wells containing Sf21 cells. The plates were kept at 27 °C, non-CO_2 atmosphere and non-humidified in New Brunswick S41i incubator shaker for 24–96 h. The cells were observed daily for morphological change; then the culture supernatants containing recombinant P1 baculoviruses were collected. SARS-CoV-2 proteins (S and M) in the culture supernatants were determined by Western blot analysis (E protein was not detected because the anti-E antibody was not available at the time this experiment was done). The concentrations/titers of individual P1 baculovirus preparations were determined by focus-forming assay (FFA). The P2 baculovirus stock was prepared by infecting the Sf21 cells with P1 baculovirus at the MOI 0.1.

The optimal ratio of the S-bacmids and ME-bacmids for the co-transfection was investigated. The Sf21 insect cells (1×10^6 cells in 200 µL of Sf-900 III SFM medium) established in individual wells of the 6-well culture plate at 27 °C, non-CO_2 atmosphere and non-humidified in the New Brunswick S41i Incubator shaker, were added with the Lipofectamine containing mixture of the S- and ME- bacmids at 1:1, 1:2, 1:3, 2:1, 2:3, 3:1 and 3:2 (total amount of bacmids in each mixture was 3 µg). The optimal ratio of the two bacmids was used for large scale production of recombinant P1 baculovirus carrying the SARS-CoV-2 S, M and E genes. Recombinant P2 baculovirus was prepared by transfecting the Sf21 cells with the P1 baculovirus at MOI 0.1.

For the separate transfection, 3 µg of S-bacmids and ME-bacmids were added separately to Lipofectamine. The Sf21 cells in different six-well culture plates were transfected separately with the Lipofectamine-bacmid mixtures, and the plates were kept at 27 °C, non-CO_2 atmosphere and non-humidified in New Brunswick S41i incubator shaker until the infected cells showed morphological change. The S-P1 baculovirus and ME-P1 baculovirus were collected from the respective cell culture supernatants. The SARS-CoV-2 proteins in the supernatants were determined by Western blot analysis. For preparing the P2 baculovirus, the S-P1 baculovirus and ME-P1 baculovirus (3 µg each) were mixed and added to the Sf21 cells in six-well culture plates at the MOI 0.1. The P2 baculovirus contained in the cell spent medium was collected.

Determination of optimal MOI for production of virus-like particles (VLPs)

Recombinant P2 baculovirus was added to Sf21 cells maintained in six-well culture plates at MOI 1, 5 and 10, and the plates were kept at 27 °C, non-CO_2 and non-humidified atmosphere for 96 h. The supernatants containing the VLPs were checked for the S, M and E proteins by Western blot analysis. Optimal MOI that gave the highest VLP yield was used for large scale production of the VLPs that contained S, M and E proteins (SME-VLPs).

Preparation of SARS-CoV-2 VLPs without furin cleavage site at the S1/S2 junction

The plasmid containing inserted SARS-CoV-2 S gene without furin cleavage site at the S1/S2 junction[33], designated S′-pFastBac1, was synthesized commercially (GenScript). The S′-pFastBac1 and the ME-plasmids were used for production of the VLPs (designated S′ME-VLPs) by means of the separate transfection using Lipofectamine as described above.

Large scale production of VLPs

Sf21 cells (2×10^6 cells/mL) were seeded into 50 mL of Sf-900 III SFM medium in 250 mL-flat bottom shake flasks. The flasks were kept at 27 °C, non-CO_2 and non-humidified atmosphere in the New Brunswick S41i Incubator shaker (125 rpm) for 30 min. Recombinant P2 baculovirus was added to the cells at optimal MOI and the flasks were kept shaking further for 96 h. The supernatant containing VLPs was filtered through sterile 0.45 µm-membrane (Pall Corporation, Port Washington, NY, USA, Catalog number: PN4614); the filtrate containing VLPs was set aside. The cell pellet was added with 20 mL NE buffer, pH 8.0 (50 mM Tris, pH 8.0, 100 mM NaCl, 1.0 mM EDTA) and the cells were lysed by five cycles of freezing (liquid nitrogen) and thawing (37 °C water-bath). After centrifugation (10,000 × *g*, 4 °C, 30 min), the supernatant containing VLPs, and the kept filtrate were combined. The preparation was concentrated by using 100-K Omega Macrosep Advance Centrifugal device (Pall Corporation, Catalog number: MAP100C37) to about 20 mL.

Purification of virus-like particles

The VLPs were purified by using HiTrap Capto CORE 400 column (Cytiva, Marlborough, USA, Catalog number: 17372411) and ÄKTA avant (Cytiva). The column was washed with 10 mL deionized water (10 column volumes) at 1 mL/min flow rate and equilibrated with 10 mL TNE buffer [50 mM Tris–HCl (pH 7.4), 100 mM NaCl, and 0.1 mM EDTA]. The concentrated VLP preparation was loaded to the column at 0.2 mL/min. The flow through fraction containing the VLPs was collected, and the column was cleaned by washing with TNE buffer containing 1.2 M NaCl. The VLPs were concentrated to 7 mL by using 100-K Omega Macrosep Advance Centrifugal device (Pall Corporation, Catalog number: MAP100C37) and overlaid onto a gradient of 20% sucrose solution (2.6 mL) and 65% sucrose solution (1.3 mL) contained in an ultracentrifuge tube (PA Thin-walled tube, Thermo Fisher Scientific, Catalog number: 03699). The tube was centrifuged at 150,000 × *g*, 4 °C for 3 h; the VLP fraction between the 20 and 60% sucrose layers was collected, added with 7 mL TNE buffer, overlaid onto 2.5 mL 20% sucrose solution in a new ultracentrifuge tube, and centrifuged (150,000 × *g*, 4 °C, 3 h). The supernatant was discarded and the pellet containing purified VLPs was added with a small volume of 0.15 M phosphate-buffered saline, pH 7.4 (PBS) (in-house preparation).

Focus-forming assay (FFA) for determination of baculovirus quantity

Sf21 cells (1×10^5 cells in 100 µL Sf-900 III SFM medium) were added to individual wells of 96-well-plate and kept at 27 °C with shaking aeration (120 rpm) and non-humidified atmosphere in a New Brunswick S41i Incubator shaker for 1 h. The recombinant baculovirus preparation was diluted 10-fold serially and 50 µL of each dilution were added to appropriate cell-containing wells (triplicate). The plates were kept as above for 1 h. The fluids in all wells were discarded and each well was added with 100 µL Sf-900 III SFM medium mixed with carboxy methyl cellulose (CMC) (Sigma-Aldrich, Darmstadt, Germany, Catalog number: C4888-500G) (0.6% CMC final concentration). The plates were incubated further for 45 h. The cells were fixed with 4% paraformaldehyde (Sigma-Aldrich, Merck, Catalog number: 158127-500G) in PBS at room temperature for 30 min, washed with 200 µL 5% normal goat serum in PBS containing 0.05% Tween-20 (PBS-T) at room temperature for 30 min. After discarding the normal goat serum, each well was added with 50 µL mouse anti-baculovirus gp64 antibody (Thermo Fisher Scientific, Catalog number: 17-6991-80). The plates were placed on a shaker (110 rpm) at 37 °C for 30 min; the cells were washed with PBS-T, added with mouse-IgGκ binding protein-horseradish peroxidase (HRP) conjugate (Santa Cruz Biotechnology, Dallas, Texas 75220, USA, Catalog number: sc-516102) and

incubated on the shaker for 30 min. The cells were washed with PBS-T before adding with 50 µL TrueBlue peroxidase substrate (KPL, Seracare, Milford, MA, USA, Catalog number: 5510-0030) to develop signal at room temperature in the dark for 2–3 h. The number of foci in each well were counted under a light microscope (100× magnification) and the focus-forming units (ffu)/mL of the baculovirus preparation was calculated: ffu/mL = (number of foci × dilution factor) / infection volume (mL).

Characterization of virus-like particles

SARS-CoV-2 proteins in the VLP preparation were analyzed by Western blotting. Each sample was added with 6× sample buffer [197.4 mM Tris pH 6.8, 6% sodium dodecyl sulfate (SDS), 60% glycerol, 0.06% bromophenol blue and 15% β-mercaptoethanol], boiled for 5 min, and subjected to sodium dodecyl sulfate-polyacrylamide gel electrophoresis (SDS-PAGE) in 4% stacking and 12% separating gels. The separated components were transblotted onto nitrocellulose (NC) membranes; the NC blots were blocked with 5% skim milk in TBS-T [0.25 M Tris-HCl (pH 7.6), 0.15 M NaCl and 0.1% Tween-20] for 1 h, washed, and submerged in solution of either mouse anti-S monoclonal antibody (in-house production), rabbit anti-SARS-CoV M protein antibody (Arigo Biolaboratories, Hsinchu City 300, Taiwan, Catalog number: ARG54884) or rabbit anti-SARS-E antibody (Abcam, Catalog number: ab272503) for detection of S, M and E proteins, respectively. After 1 h, the NC membranes were washed with TBS-T and placed into a solution of secondary antibodies, i.e., goat-anti-rabbit immunoglobulin (Ig)-HRP conjugate (Southern Biotech, Birmingham, AL 35209, USA, Catalog number: 4030-05) and mouse-IgGκ binding protein-HRP conjugate (Thermo Scientific). After 1 h, the NC membranes were washed with TBS-T and the color signal was developed by using Immobilon Forte Western HRP substrate (Merck, Catalog number: WBLUF0100). The antigen-antibody reactive bands were visualized by using ImageQuant LAS 4010 (GE Healthcare, Cytiva).

The VLPs were negatively stained by uranyl acetate and observed under transmission electron microscopy (TEM) for their apparent morphology. The VLP sizes and surface charges were determined by using dynamic light scattering (DLS)-zetasizer (Malvern, DKSH, Zurich, Switzerland).

Preparation of liposome and formulation of liposome-adjuvanted VLP vaccines

Multilamellar liposome was prepared as described previously[53] from mixture of 148 mg phosphatidylcholine (LIPOID S 100; LIPOID AG, CH – 6312 Steinhausen, Switzerland, Catalog number: 97281-47-5) and 72.5 mg cholesterol (Merck, Catalog number: 228111) using 153 mg dodecyl dioctadecyl ammonium bromide (DDAB, Sigma-Aldrich, Merck, Catalog number: 359025) as a cationic surfactant and 25 mL dichloromethane (Sigma-Aldrich, Merck, Catalog number: 106050) as a solvent. A film of 1 mL lipid stock (30 µM) was made on the inner surface of a round-bottom flask; then, 240 µg of VLPs (SME-VLPs/S′ME-VLPs) in 800 µL PBS were added to the lipid film and mixed until a homogeneous creamy preparation was obtained. Liposome-adjuvanted VLP vaccines were prepared. For placebo, PBS was used instead of the VLPs for preparing liposome-entrapped PBS (L-PBS).

Mouse immunization and vaccine innocuity and immunogenicity

Female BALB/c mice, 5 weeks old, were purchased from Nomura Siam International, Bangkok, Thailand. Mice were accustomed in the animal facility of the Faculty of Medicine Siriraj Hospital, Mahidol University, Bangkok, before commencing the experiments. Each mouse was bled (submandibular) to collect preimmunized serum sample. They were divided into 6 mice per group.

For experiment 1, mice were divided into three groups. Mice of group 1 (T1-T6) received IP three doses of the L-SME-VLPs vaccine (100 µL of vaccine containing 30 µg SME-VLPs) at two-week intervals. Mice of group 2 (T7-T12) received IP three doses of the L-S′ME-VLPs vaccine (100 µL of vaccine containing 30 µg S′ME-VLPs), and mice of group 3 (C1-C6) received three doses of placebo (100 µL of L-PBS), also at two-weeks apart. Fourteen days post last booster, the mice were bled and euthanized. Specific antibodies to SARS-CoV-2 S1 protein in all mouse serum samples were determined by indirect ELISA. The virus-neutralizing (VN) antibody titers were measured by microneutralization test performed in BSL-3 laboratory. Gross appearances of internal organs including spleens, kidneys, livers and lungs of all mice were observed and their sizes were measured and photographed. Spleens were placed in RNA later solution (Invitrogen, Thermon Fisher Scientific, Catalog number: AM7024) for cytokine mRNAs determination by qRT-PCR using oligonucleotide primers as shown in Table S3.

For the second experiment, mice of group 1 (T13-T18) and group 2 (T19-T24) were immunized intranasally (IN) with L-SME-VLP and S′ME-VLPs (50 µL of vaccine containing 30 µg of SME-VLPs/S′ME-VLPs; 25 µL per nostril), respectively, at two-weeks intervals. Mice of group 3 (C7-C12) were administered IN with 50 µL of L-PBS (25 µL per nostril) using the same timeline as the first experiment (Supplementary Fig. S2). Two weeks after the third dose, bronchoalveolar lavage fluid (BALF) was collected from each mouse after euthanasia by flushing the respiratory tract with 1 mL PBS. ELISA and VN titers (FFA) in BALF samples against S1 protein and the antibody isotypes were determined. Internal organs of all mice were observed as for the first experiment.

Indirect enzyme-linked immunosorbent assay (indirect ELISA)

Recombinant S1 of SARS-CoV-2 Wuhan wildtype (in-house production from transformed *E. coli*) was used to coat wells of a 96-well microplate (Nunc, Thermo Fisher Scientific, Catalog number: 44-2404) (0.5 µg in 100 µL bicarbonate buffer, pH 9.6, per well) and kept at 4 °C overnight. All wells were blocked with 300 µL of 3% BSA in PBS-T at 37 °C for 1 h. After washing the wells with PBS-T to discard excess blocking protein, diluted samples (100 µL) were added to appropriate antigen-coated wells and the plates were kept at 30 °C for 1 h. After washing with PBS-T, wells were added with 100 µL goat-anti mouse Ig-HRP conjugate (Southern Biotech, Catalog number: 1036-05; diluted 1:3000 with PBS-T) and incubated at 37 °C for 1 h. ABTS [2,2′-azinobis

(3-ethylbenzothiazoline-6-sulfonic acid)] substrate (100 µL; KPL, Seracare, Catalog number: 5120-0041) was used for color development at room temperature in the dark for 30 min. The enzymatic reaction was stopped by adding 100 µL of 1 M orthophosphoric acid. Optical density at 405 nm (OD405) of contents in all wells were determined by using BioTek Synergy H1 microplate reader (Biotek, Sata Clara, CA, USA).

Antibody isotyping

Isotypes of antibodies to SARS-CoV-2 S1 protein in mouse samples were determined by using Ig isotyping mouse uncoated ELISA kit (Invitrogen, Catalog number: 88-50630-88). The wells of ELISA plate were coated with recombinant S1 and the empty sites on the well surface were blocked as above. The samples were added to appropriate coated wells, and the plates were incubated at 37 °C for 1 h. After washing, rat anti-mouse Ig isotypes (IgG1, IgG2a, IgG2b, IgG3, IgA, IgM, κ light chain, λ light chain) were added to appropriate wells and incubated at 37 °C for 1 h. Thereafter, wells were washed with PBS-T before adding with 100 µL goat anti-rat Ig-HRP conjugate (Southern Biotech; diluted 1:3000 in PBS-T), kept at 37 °C for 1 h, washed again with PBS-T, and added each well with SureBlue TMB 1-Component Microwell Peroxidase Substrate (3,3′,5,5′- tetramethylbenzidine) (KPL, Seracare, Catalog number: 5120-0075). The plate was kept at room temperature in the dark for 30 min. OD450 of the content in each well was determined (BioTek Synergy H1).

Microneutralization assay

Vero E6 cells (4×10^4 cells) were seeded to 96-well culture plate and incubated at 37 °C in 5% CO_2 atmosphere overnight. Mouse serum samples were diluted two-fold serially; each dilution (60 µL) was mixed with SARS-CoV-2 (100 PFU/60 µL) and incubated at 37 °C for 1 h. The mixtures were added to the cells in appropriate wells and incubated at 37 °C with 5% CO_2 for 1 h. The supernatant was replaced with DMEM containg 2% FBS. All plates were incubated at 37 °C for 72 h. The cells in all wells were washed twice with PBS and fixed with 4% paraformaldehyde solution at room temperature for 20 min. After washing and blocking with 5% skim milk in PBS, mouse anti-S1 antibody (in-house preparation) was added, incubated at room temperature for 1 h, washed with PBS and added with goat-anti mouse Ig-HRP conjugate (Southern Biotech, Catalog number: 1036-05; diluted 1:3000 in PBS). After washing, the SureBlue TMB 1-Component Microwell Peroxidase Substrate (KPL, Seracare, Catalog number: 5120-0075) was added and the plates were kept in darkness for 30 min. The foci were obseverd and counted under inverted microscope (100×).

Quantitative resverse transcription-polymerase chain reaction (qRT-PCR) for determining expression of cytokine genes in the mouse spleens

The total RNA were extracted form spleens of individual mice of all groups by using TRIzol Reagent (Invitrogen, Thermo Fisher Scientific, Catalogue Number: 15596026). Each mouse spleen (50–100 mg) added with 1 mL of TRIzol Reagent was ground by using micropestle and incubated at room temperature for 5 min before adding with 0.2 mL of chloroform, mixed by shaking, and centrifuged (12,000 × *g*, 4 °C, 15 min). The aqueous phase was transferred to 1.5 mL microcentrifuge tube, added with 0.5 mL of isopropanal and kept at 4°C for 10 min. The preparation was centrifuged (12,000 × g, 4 °C, 15 min); the supernatant was discarded and the RNA pellet was washed with 500 µL of 75% ethanol. After drying, the RNA was dissolved in 35 µL of nuclease-free water and incubated at 60 °C for 10 min. The RNA concentration was measured by Nanodrop.

Expression of genes coding cytokines including IFN-γ, TNF-α, TGF-β, IL-2, IL-4, IL-5, IL-10, IL-12, IL-13 and IL-17 was determined by using the qRT-PCR Brilliant III SYBR Master Mix (Agilent, Agilent technologies, Stevens Creek Blvd Santa Clara, California, USA, Catalogue Number: 600887). The primers for cytokine genes and control house-keeping gene are listed in Supplementary Table S3. Expression of cytokines (mRNAs) were calculated from the Ct value using a $2^{-\Delta\Delta Ct}$ method in relation to the mRNAs of the control mice that received placebo.

Statistical analysis

The mean values and standard deviations (SD) between groups were compared using non-parametric Kruskal-Wallis test (GraphPad Prism version 9 software, GraphPad Software, San Diego, CA, USA). *P*-value of 0.05 or lower was considered statistically significant: $p > 0.05$ (ns, not significant); $p < 0.05$ (*), $p < 0.01$ (**), $p < 0.0001$ (****).

Statement of approval

Animal experiments received ethical approval from Animal Care and Use Committee (ACUC), Faculty of Medicine Siriraj Hospital, Mahidol University, Bangkok (No. 013/2563). Biological safety experiments were approved by Siriraj Safety Risk Management Taskforce, Mahidol University (No. SI 2020-033). All experiments in this study are reported in accordance with the ARRIVE guidelines.

Data availability

The data supporting this study's findings are presented within the manuscript and its supplementary materials. Additional raw data and detailed protocols are available from the corresponding author upon reasonable request, subject to data sharing agreements.

Received: 6 August 2024; Accepted: 6 November 2024
Published online: 09 November 2024

References

1. Alu, A. et al. Intranasal COVID-19 vaccines: From bench to bed. *EBioMedicine* **76**, 103841. https://doi.org/10.1016/j.ebiom.2022.103841 (2022).
2. Brisse, M., Vrba, S. M., Kirk, N., Liang, Y. & Ly, H. Emerging concepts and technologies in vaccine development. *Front. Immunol.* **11**, 583077. https://doi.org/10.3389/fimmu.2020.583077 (2020).
3. Sharifzadeh, M., Mottaghi-Dastjerdi, N. & Soltany, R. R. M. A review of virus-like particle-based SARS-CoV-2 vaccines in clinical trial phases. *Iran. J. Pharm. Res.* **21**, e1270422022. https://doi.org/10.5812/ijpr-127042 (2022).
4. Russell, M. W. & Mestecky, J. Mucosal immunity: The missing link in comprehending SARS-CoV-2 infection and transmission. *Front. Immunol.* **13**, 957107. https://doi.org/10.3389/fimmu.2022.957107 (2022).
5. Lycke, N. Recent progress in mucosal vaccine development: Potential and limitations. *Nat. Rev. Immunol.* **12**, 592–605. https://doi.org/10.1038/nri3251 (2012).
6. Fraser, R., Orta-Resendiz, A., Mazein, A. & Dockrell, D. H. Upper respiratory tract mucosal immunity for SARS-CoV-2 vaccines. *Trends Mol. Med.* **29**, 255–267. https://doi.org/10.1016/j.molmed.2023.01.003 (2023).
7. Russell, M. W. & Mestecky, J. Mucosal vaccines: Overview. In: Mestecky J, Strober W, Russell MW, Kelsall BL, Cheroutre H, Lambrecht BN, editors. *Mucosal Immunology*, 4th edition 1039–1046. (Academic Press/Elsevier, 2015).
8. Li, M. et al. Mucosal vaccines: Strategies and challenges. *Immunol. Lett.* **217**, 116–125. https://doi.org/10.1016/j.imlet.2019.10.013 (2020).
9. Langel, S. N. et al. Adenovirus type 5 SARS-CoV-2 vaccines delivered orally or intranasally reduced disease severity and transmission in a hamster model. *Sci. Transl. Med.* **14**, eabn6868. https://doi.org/10.1126/scitranslmed.abn6868 (2022).
10. Zhang, H., Wang, H., An, Y. & Chen, Z. Construction and application of adenoviral vectors. *Mol. Ther. Nucleic Acids*. **34**, 102027. https://doi.org/10.1016/j.omtn.2023.09.004 (2023).
11. Lei, H. et al. Cationic crosslinked carbon dots-adjuvanted intranasal vaccine induces protective immunity against Omicron-included SARS-CoV-2 variants. *Nat. Commun.* **14**. https://doi.org/10.1038/s41467-023-38066-8 (2023).
12. Liu, J. et al. Rapid degradation of SARS-CoV-2 spike S protein by a specific serine protease. *Molecules* **27**, 1882. https://doi.org/10.3390/molecules27061882 (2022).
13. Recombinant, S. A. R. S. S1 subunit protein (RBD) with c-terminal his-tag, transfected HEK293 cell culture supernatant. https://www.raybiotech.com/recombinant-sars-cov-2-s1-subunit-protein-rbd-with-c-terminal-his-tag-transfected-hek293-cell-culture-supernatant-230-20406-200. Accessed 5 July 2024.
14. Recombinant, S. A. R. S. July CoV-2 spike his protein. (2024). https://www.novusbio.com/products/recombinant-sars-cov-2-spike-his-protein-cf_10549-cv. Accessed 5.
15. Roldão, A., Silva, A. C., Mellado, M. C. M., Alves, P. M. & Carrondo, M. J. T. Viruses and virus-like particles in biotechnology: Fundamentals and applications. *Compr. Biotechnol. P.* 633–656. https://doi.org/10.1016/b978-0-12-809633-8.09046-4 (2017).
16. SARS-CoV-2 virus-like particles. https://www.leadgenebio.com/sars-cov-2-virus-like-particles-ldg002pvm.html. Accessed 5 July 2024.
17. Laue, M. et al. Morphometry of SARS-CoV and SARS-CoV-2 particles in ultrathin plastic sections of infected Vero cell cultures. *Sci. Rep.* **11**, 3515. https://doi.org/10.1038/s41598-021-82852-7 (2021).
18. Oyewumi, M. O., Kumar, A. & Cui, Z. Nano-microparticles as immune adjuvants: Correlating particle sizes and the resultant immune responses. *Expert Rev. Vaccines*. **9**, 1095–1107. https://doi.org/10.1586/erv.10.89 (2010).
19. Mumper, R. J., Cui, Z. & Oyewumi, M. O. Nanotemplate engineering of cell specific nanoparticles. *J. Dispers Sci. Technol.* **24**, 569–588. https://doi.org/10.1081/DIS-120021814 (2003).
20. Monfardini, C. & Veronese, F. M. Stabilization of substances in circulation. *Bioconjug. Chem.* **9**, 418–450. https://doi.org/10.1021/bc970184f (1988).
21. Xiang, S. D. et al. Pathogen recognition and development of particulate vaccines: Does size matter? *Methods* **40**, 1–9. https://doi.org/10.1016/j.ymeth.2006.05.016 (2006).
22. Kanchan, V. & Panda, A. K. Interactions of antigen-loaded polylactide particles with macrophages and their correlation with the immune response. *Biomaterials* **28**, 5344–5357. https://doi.org/10.1016/j.biomaterials.2007.08.015 (2007).
23. Tseng, C. T. et al. Immunization with SARS coronavirus vaccines lead to pulmonary immunopathology on challenge with the SARS virus. *PLoS One* **7**, e35421. https://doi.org/10.1371/journal.pone.0035421 (2012).
24. Waris, M. E., Tsou, C., Erdman, D. D., Zaki, S. R. & Anderson, L. J. Respiratory syncytial virus infection in BALB/c mice previously immunized with formalin-inactivated virus induces enhanced pulmonary inflammatory response with a predominant Th2-like cytokine pattern. *J. Virol.* **70**, 2852–2860. https://doi.org/10.1128/JVI.70.5.2852-2860.199 (1996).
25. Gall, D. The adjuvant activity of aliphatic nitrogenous bases. *Immunology*. **11**, 369–386 (1966).
26. Wang, N., Chen, M. & Wang, T. Liposomes used as a vaccine adjuvant-delivery system: From basics to clinical immunization. *J. Control Release* **303**, 130–150. https://doi.org/10.1016/j.jconrel.2019.04.025 (2019).
27. Leal, J., Smyth, H. D. C. & Ghosh, D. Physicochemical properties of mucus and their impact on transmucosal drug delivery. *Int. J. Pharm.* **532**, 555–572. https://doi.org/10.1016/j.ijpharm.2017.09.018 (2017).
28. Power, U. F. et al. Induction of protective immunity in rodents by vaccination with a prokaryotically expressed recombinant fusion protein containing a respiratory syncytial virus G protein fragment. *Virology* **230**, 155–166. https://doi.org/10.1006/viro.1997.8465 (1997).
29. Gautam, A. et al. Peritoneal cells mediate immune responses and cross-protection against influenza a virus. *Front. Immunol.* **10**, 1160. https://doi.org/10.3389/fimmu.2019.01160 (2019).
30. Lei, Z. et al. J. A vaccine delivery system promotes strong immune responses against SARS-CoV-2 variants. *J. Med. Virol.* **95**, e28475. https://doi.org/10.1002/jmv.28475 (2023).
31. Krist, L. F. et al. Cellular composition of milky spots in the human greater omentum: an immunochemical and ultrastructural study. *Anat. Rec.* **241**, 163–174. https://doi.org/10.1002/ar.1092410204 (1995).
32. Rangel-Moreno, J. et al. Omental milky spots develop in the absence of lymphoid tissue-inducer cells and support B and T cell responses to peritoneal antigens. *Immunity* **30**, 731–743 ; (2009). https://doi.org/10.1016/j.immuni.2009.03.014
33. Bertrand, Y., Sánchez-Montalvo, A., Hox, V., Froidure, A. & Pilette, C. IgA-producing B cells in lung homeostasis and disease. *Front. Immunol.* **14**, 1117749. https://doi.org/10.3389/fimmu.2023.1117749 (2023).
34. Kroese, F. G. et al. Many of the IgA producing plasma cells in murine gut are derived from self-replenishing precursors in the peritoneal cavity. *Int. Immunol.* **1**, 75–84. https://doi.org/10.1093/intimm/1.1.75 (1989).
35. Kawahara, T., Ohdan, H., Zhao, G., Yang, Y. G. & Sykes, M. Peritoneal cavity B cells are precursors of splenic IgM natural antibody-producing cells. *J. Immunol.* **171**, 5406–5414. https://doi.org/10.4049/jimmunol.171.10.5406 (2003).
36. Kaminski, D. A. & Stavnezer, J. Enhanced IgA class switching in marginal zone and B1 B cells relative to follicular/B2 B cells. *J. Immunol.* **177**, 6025–6029. https://doi.org/10.4049/jimmunol.177.9.6025 (2006).
37. Papa, G., James, L. C. et al. Furin cleavage of SARS-CoV-2 spike promotes but is not essential for infection and cell-cell fusion. *PLoS Pathog.* **17**, e1009246. https://doi.org/10.1371/journal.ppat.1009246 (2021).
38. Damelang, T., Rogerson, S. J., Kent, S. J. & Chung, A. W. Role of IgG3 in infectious diseases. *Trends Immunol.* **40**, 197–211. https://doi.org/10.1016/j.it.2019.01.005 (2019).
39. Kim, D. M. et al. Enhanced eosinophil-mediated inflammation associated with antibody and complement-dependent pneumonic insults in critical COVID-19. *Cell Rep.* **37**, 109798 (2021). https://doi.org/10.1016/j.celrep.2021.109798

40. Birkhoff, M., Leitz, M. & Marx, D. Advantages of intranasal vaccination and considerations on device selection. *Indian J. Pharm. Sci.* **71**, 729–731 (2009).
41. Xing, M. et al. Zhou, D. An intranasal combination vaccine induces systemic and mucosal immunity against COVID-19 and influenza. *NPJ Vaccines* **9**, 64. https://doi.org/10.1038/s41541-024-00857-5 (2024).
42. Sindhava, V. J. & Bondada, S. Multiple regulatory mechanisms control B-1 B cell activation. *Front. Immunol.* **3**, 372. https://doi.org/10.3389/fimmu.2012.00372 (2012).
43. Kawai, A. et al. Intranasal immunization with an RBD-hemagglutinin fusion protein harnesses preexisting immunity to enhance antigen-specific responses. *J. Clin. Invest.* **133**, e166827. https://doi.org/10.1172/JCI166827 (2023).
44. Michaelsen, T. E., Kolberg, J., Aase, A., Herstad, T. K. & Høiby, E. A. The four mouse IgG isotypes differ extensively in bactericidal and opsonophagocytic activity when reacting with the P1.16 epitope on the outer membrane PorA protein of *Neisseria meningitidis*. *Scand. J. Immunol.* **59**, 34–39. https://doi.org/10.1111/j.0300-9475.2004.01362.x (2004).
45. Hocart, M. J., Mackenzie, J. S. & Stewart, G. A. The immunoglobulin G subclass responses of mice to influenza a virus: The effect of mouse strain, and the neutralizing abilities of individual protein A-purified subclass antibodies. *J. Gen. Virol.* **70**, 2439–2448. https://doi.org/10.1099/0022-1317-70-9-2439 (1989).
46. LeClerc, C. et al. Induction of virus-neutralizing antibodies by bacteria expressing the C3 poliovirus epitope in the periplasm. The route of immunization influences the isotypic distribution and the biologic activity of the anti-poliovirus antibodies. *J. Immunol.* **144**, 3174–3182 (1990).
47. Monteyne, P. & Coutelier, J. P. Difference in neutralization between lactate dehydrogenase-elevating virus isolated from acutely and chronically infected mice. *J. Gen. Virol.* **75**, 1173–1176. https://doi.org/10.1099/0022-1317-75-5-1173 (1994).
48. Smucny, J. J., Kelly, E. P., Macarthy, P. O. & King, A. D. Murine immunoglobulin G subclass responses following immunization with live dengue virus or a recombinant dengue envelope protein. *Am. J. Trop. Med. Hyg.* **53**, 432–437. https://doi.org/10.4269/ajtmh.1995.53.432 (1995).
49. Markine-Goriaynoff, D. & Coutelier, J. P. Increased efficacy of the immunoglobulin G2a subclass in antibody-mediated protection against lactate dehydrogenase-elevating virus-induced polio encephalomyelitis revealed with switch mutants. *J. Virol.* **76**, 432–435. https://doi.org/10.1128/jvi.76.1.432-435.2002 (2002).
50. Boyaka, P. N. Inducing mucosal IgA: A challenge for vaccine adjuvants and delivery systems. *J. Immunol.* **199**, 9–16. https://doi.org/10.4049/jimmunol.1601775 (2017).
51. Skwarczynski, M. & Toth, I. Non-invasive mucosal vaccine delivery: Advantages, challenges and the future. *Expert Opin. Drug Deliv*. **17**, 435–437. https://doi.org/10.1080/17425247.2020.1731468 (2020).
52. Glab-ampai, K. et al. Human superantibodies to $3CL^{pro}$ inhibit replication of SARS-CoV-2 across variants. *Int. J. Mol. Sci.* **23**, 6587. https://doi.org/10.3390/ijms23126587 (2022).
53. Meechan, P. et al. Intranasal, liposome-adjuvanted cockroach allergy vaccines made of refined major allergen and whole-body extract of *Periplaneta americana*. *Int. Arch. Allergy Immunol.* **161**, 351–362. https://doi.org/10.1159/000348314 (2013).

Acknowledgements

The authors thank Professor Dr. Prasert Auewarakul and colleagues, Department of Microbiology, Faculty of Medicine Siriraj Hospital, Mahidol University, Bangkok 10700, Thailand for providing SARS-CoV-2 wildtype strain Si and Vero E6 cells.

Author contributions

WC conceived the research project, acquired research grant and wrote the manuscript. WC, KG and MC designed the experiments and analyzed the data. MC, KG, PP, and KM performed the experiments. KG and MC prepared Figures.

Funding

The authors gratefully acknowledge the support from the Government Pharmaceutical Organization (GPO) of Thailand (grant no. 07/2563) and Mahidol University, Thailand (grant no. MU-SRF-PF-06 C/66).

Declarations

Competing interests

The authors declare no competing interests.

Additional information

Supplementary Information The online version contains supplementary material available at https://doi.org/10.1038/s41598-024-79122-7.

Correspondence and requests for materials should be addressed to K.G.-a.